

# Theoretical and experimental study of fine erbium oxide powder treatment in RF plasma jet to obtain light-emitting microspheres

© V.A. Sergeev<sup>1</sup>, S.G. Zverev<sup>1</sup>, S.Yu. Grachev<sup>1</sup>, A.V. Medvedev<sup>2</sup>, D.V. Ivanov<sup>1</sup>, A.A. Mashigin<sup>1</sup>

<sup>1</sup> Peter the Great Saint-Petersburg Polytechnic University, St. Petersburg, Russia

<sup>2</sup> Ioffe Institute, St. Petersburg, Russia

E-mail: d.ivanov@spbstu.ru

Received May 5, 2025

Revised June 27, 2025

Accepted July 7, 2025

Mathematical modeling of processes in a RF inductively coupled plasma torch is described. The obtained temperature and plasma velocity distributions were used as initial data for calculating the motion of erbium oxide powder in a plasma jet. As a result, the technological process parameters were obtained that ensure effective processing. The obtained operating parameters were used for experimental studies. The obtained erbium oxide microspheres turned out to be an order of magnitude larger than the initial powder. The article presents hypotheses explaining this result. Optical studies of the obtained microspheres showed intense photoluminescence in the visible and near infrared spectral range.

**Keywords:** erbium oxide, light-emitting microspheres, plasma treatment, RF inductively coupled plasma torch

DOI: 10.61011/TPL.2025.12.62782.8053

Rare earth metal oxides, of which erbium oxide ( $\text{Er}_2\text{O}_3$ ) is an example, attract attention due to such properties as high transparency in a wide spectral region (from UV to IR) and a fairly high refraction index. Materials based on  $\text{Er}_2\text{O}_3$  are used in optoelectronic devices as converters of IR radiation into visible light (upconversion [1]), for fabrication of color displays [2], etc. The properties of such a material are closely related to its size and shape.

Specifically, the spherical shape of  $\text{Er}_2\text{O}_3$  particles helps reduce radiation losses due to light scattering and allows one to use them as an active core in spherical Bragg reflectors [3,4]. Such structures may be used to control spontaneous emission [5] and design low-threshold omnidirectional microlasers [6,7]. However, the production of microspheres of the size suitable for lasing (on the order of  $100\ \mu\text{m}$ ) is associated with technological difficulties. For example, the microspheres obtained by chemical means in [8] had a diameter of just  $0.2\text{--}0.3\ \mu\text{m}$ , and irregularly shaped quasi-microspheres in [9] were no larger than  $3\ \mu\text{m}$ . The typical surface quality of such microspheres is very low, since their structure may be riddled with holes and cavities and their surface is uneven. In addition, microspheres may get stuck together and form agglomerates.

Therefore, the task of synthesizing sufficiently large (up to  $100\ \mu\text{m}$ ) erbium oxide microspheres remains relevant. The conditions necessary for obtaining such powders are chemical purity and high temperature of the working medium, since erbium oxide is a refractory material.

In the present study, we propose to synthesize  $\text{Er}_2\text{O}_3$  microspheres in a plasma jet generated by a radio-frequency inductively coupled (RFIC) plasma torch [10–12]. The starting material in this case is fine  $\text{Er}_2\text{O}_3$  powder of

particles with an average diameter on the order of  $1\ \mu\text{m}$ , which form large agglomerates up to  $200\ \mu\text{m}$  in size.

The following features of RF ICP torches make them well suited for use as high-temperature jet sources: the chemical purity of plasma due to a lack of electrodes; the capacity to produce plasma from gas of any composition, which helps avoid unwanted chemical reactions; and the large volume and low velocity of a plasma jet, which have a positive effect on powder processing performance.

Electromagnetic, thermal, and gasdynamic processes proceed inside the RF ICP torch. In much the same way as in transformer operation and inductive heating of metals, alternating current is passed through an inductor, which produces an alternating magnetic field in the surrounding space. This field induces ring current in the core of plasma in the plasma torch tube, which leads to the release of thermal power that is needed to maintain it. Cold gas enters the plasma torch, is heated by the plasma core and transitions to a plasma state, is accelerated, and flows out through the outlet section of the plasma torch, forming a plasma jet. All these processes are characterized by the model detailed in [13–16]. The problem was solved in a two-dimensional axisymmetric formulation in COMSOL Multiphysics. The distributions of temperature, velocity, pressure, electric and magnetic field strength, and other electromagnetic quantities were determined as a result of calculation. This allowed us to evaluate the efficiency of the given operating mode of the plasma torch. In addition, the obtained plasma temperature and velocity distributions in the outlet section of the plasma torch were used as initial data for calculating the motion of erbium oxide powder in the plasma jet.

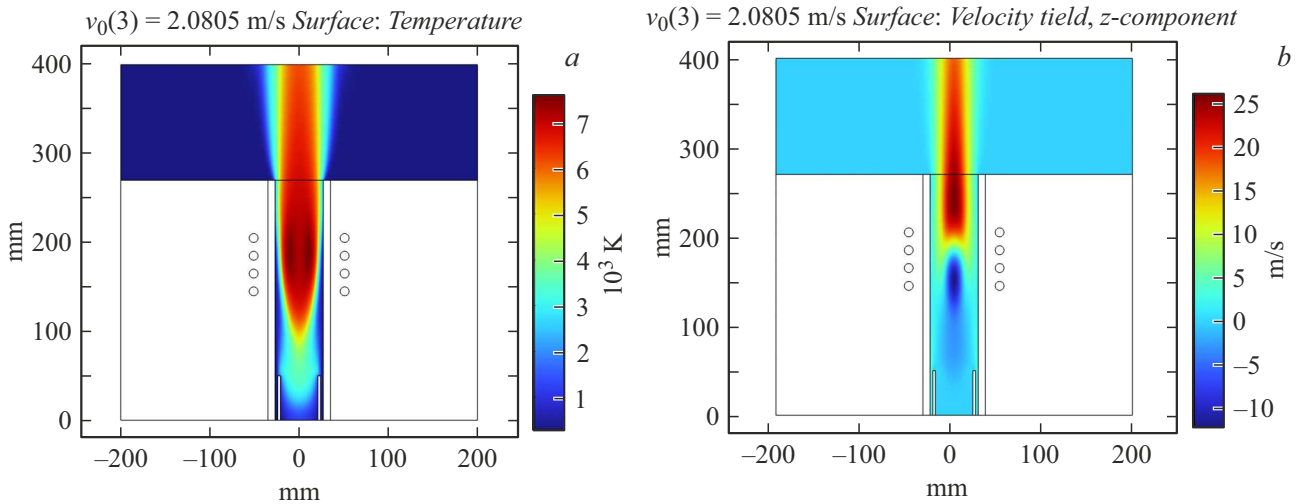


**Figure 1.** Results of mathematical modeling of plasma processes in an RF ICP torch. *a* — plasma temperature distribution; *b* — plasma axial velocity distribution.

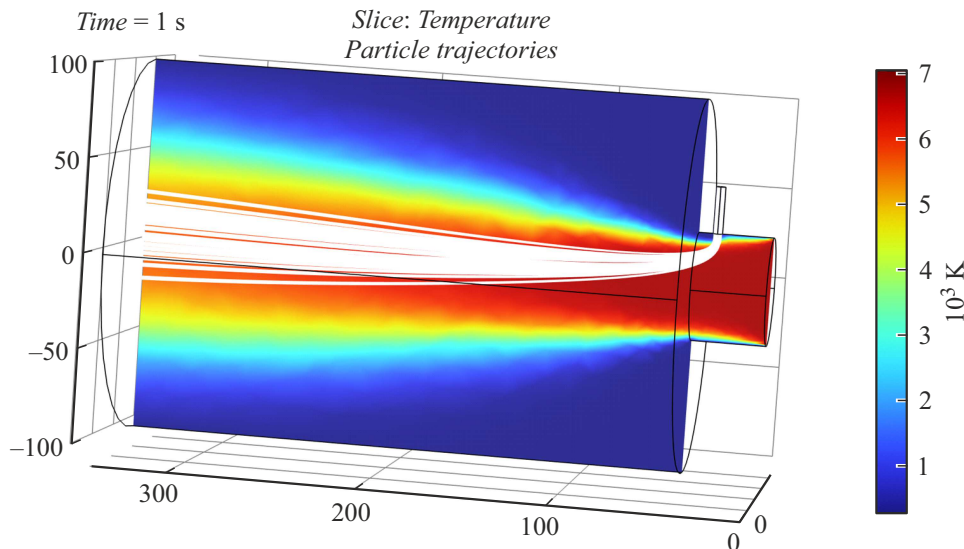


**Figure 2.** Results of calculation of motion of fine erbium oxide powder in a plasma jet.

The calculation of particle motion in a plasma jet was described in detail in [13]. The problem was solved in a three-dimensional non-stationary formulation in COMSOL Multiphysics.

The RF ICP torch with an internal tube diameter of 54 mm operating at a frequency of 5.28 MHz was used for studies. The power input into plasma may vary within the range of 20–40 kW; in calculations and experiments, the plasma power was 30 kW. The inductor had four turns, an internal diameter of 92 mm, and a height of 70 mm. The geometry is detailed in [17]. Air was the plasma-forming gas; its flow rate was 60 l/min. The plasma torch had an angle of inclination to the horizon of  $20^\circ$  (this was not taken into account in calculations).

A feeder tube was positioned at a distance of 30 mm from the outlet section of the plasma torch. Erbium oxide powder was fed through it from top to bottom at a rate of 0.1 kg/h.

The above-described RF ICP torch was used in experiments. The device itself and its power supply are located in the Laboratory of Radio-Frequency Plasma Technology at Peter the Great St. Petersburg Polytechnic University.

Experiments were aimed at investigating the possibility of production of light-emitting erbium oxide microspheres from the initial fine powder.

Video recording with an EVERCAM 2000-16-C high-speed camera [18] was performed additionally to examine the details of processing visually.

Figure 1 shows the distributions of temperature and plasma velocity inside the RF ICP torch obtained in calculations.

The maximum plasma temperature is 7606 K. It can be seen that the region of maximum temperature is shifted away from the axis, which is typical of induction heating devices. The maximum axial plasma velocity is

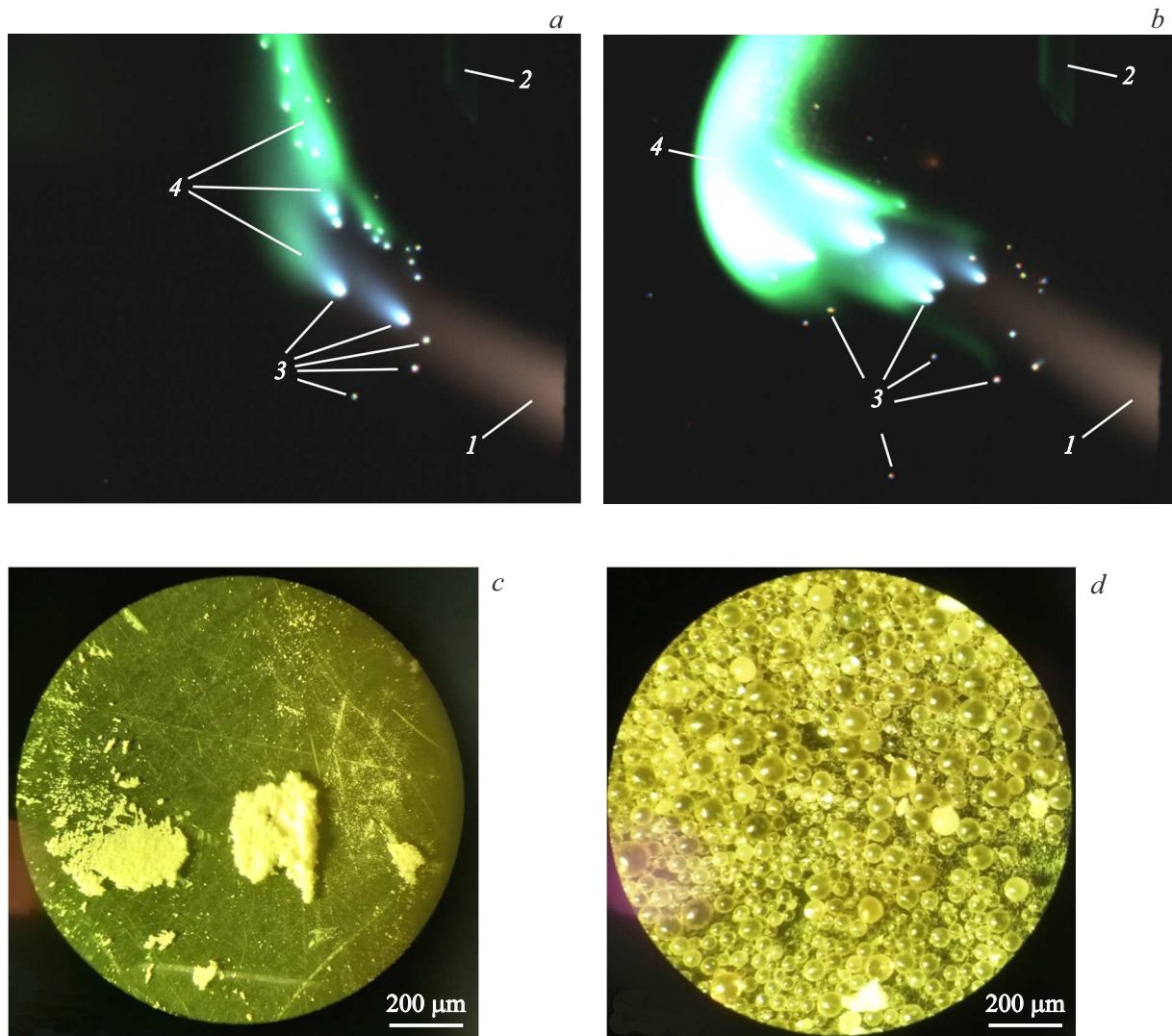


**Figure 3.** Experimental studies of erbium oxide powder processing in a plasma jet. *a, b* — high-speed video frames illustrating erbium oxide powder processing in an RF plasma jet. *1* — plasma jet, *2* — quartz tube for powder feeding, *3* — powder particles, and *4* — erbium oxide vapor. *c, d* — erbium oxide powder imaged with a microscope before and after processing, respectively.

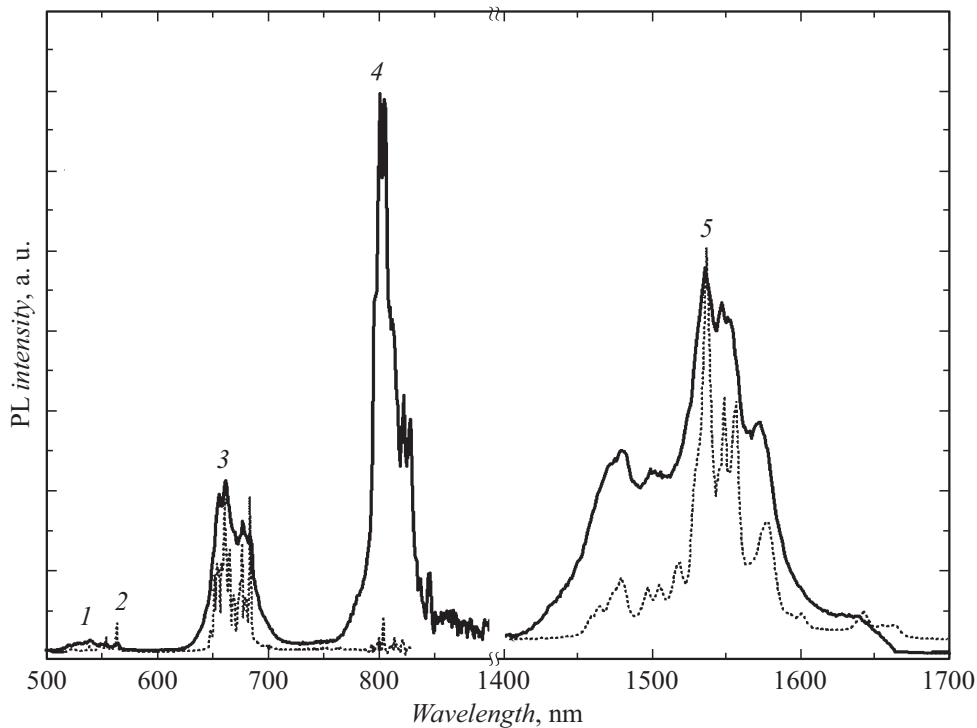
26.3 m/s. Since the velocity is this low (compared to arc plasma, where typical velocities are at least an order of magnitude higher), the residence time of the powder fed into the plasma jet is quite long (tens of milliseconds). This, in turn, leads to more efficient heating of the powder.

Figure 2 shows the trajectories of motion of erbium oxide powder particles in the plasma jet. Efficient processing requires that powder particles (in the calculation, the average powder diameter was set to  $80\ \mu\text{m}$ ) be moving in the axial region of the plasma jet, where temperature is the highest. A corresponding mode was found; it is established at an initial particle velocity of 5 m/s.

Figures 3, *a, b* show high-speed video frames illustrating erbium oxide powder processing in the RF plasma jet. The operating mode is as follows: plasma power, 30 kW, plasma-

forming gas flow rate, 60 l/min; powder consumption, 0.1 kg/h; transport gas flow rate, 5 l/min. High-speed video recording mode: 4000 fps; exposure time, 1/4000 s. The presented images were recorded through a K&F Concept Variable MC ND8-ND2000 neutral density filter at maximum attenuation (2000). Plasma jet *1* and quartz tube *2* for powder feeding are seen in the bottom right and top right corners, respectively. Since particles heated to a high temperature glow brighter than plasma, bright dots *3* seen in the high-speed video frames are the particles being processed. If particles are exposed to high temperatures for a sufficiently long time, a brightly glowing cloud (*4*) forms around them and is carried away by the plasma jet. This is erbium oxide vapor (particles evaporate in part).

Figures 3, *c, d* present optical photographs of erbium oxide powder. The average particle diameter is  $1\ \mu\text{m}$



**Figure 4.** PL spectra of erbium oxide powder after processing. The dashed and solid curves represent the PL spectra of an individual erbium oxide particle and a microsphere. Numbers denote transitions: 1 and 2 —  $^2H_{11/2} \rightarrow ^4I_{15/2}$  and  $^4S_{3/2} \rightarrow ^4I_{15/2}$  (530, 550 nm), 3 —  $^4F_{9/2} \rightarrow ^4I_{15/2}$  (660 nm), 4 —  $^4I_{9/2} \rightarrow ^4I_{15/2}$  (800 nm), 5 —  $^4I_{13/2} \rightarrow ^4I_{15/2}$  (1540 nm).

(particle agglomerates are as large as  $200\ \mu\text{m}$ ) prior to processing and  $20\text{--}80\ \mu\text{m}$  after processing (particle-size distribution:  $20\text{--}80\ \mu\text{m}$  — 60%, smaller than  $20\ \mu\text{m}$  — 25%, larger than  $80\ \mu\text{m}$  — 15%; no hollow microspheres are seen; the photograph also reveals an insignificant (in mass) fraction of original particles with a diameter of  $\sim 1\ \mu\text{m}$ ). Thus, the obtained erbium oxide microspheres turned out to be an order of magnitude larger than the original powder particles. The reason for this is not entirely clear. Let us list feasible hypotheses.

1. Original particles enter plasma in an agglomerated form, melt, and merge in the liquid phase under the action of surface tension forces into a larger particle, which then solidifies into a microsphere upon leaving the plasma jet. It is known that under certain conditions, hollow microspheres with characteristic small wall thicknesses (compared to the particle diameter) are produced during plasma treatment of agglomerated particles [19,20], and the product also contains a certain number of broken shells. Since this is not seen in Fig. 3, *d*, it can be concluded that the produced microspheres are solid.

2. Original particles enter plasma and are evaporated due to their small size. Erbium oxide vapor then moves in the plasma jet and cools after leaving it. In this case, spherical microspheres are formed by condensation of erbium oxide vapor. This process is somewhat similar

to the synthesis of nanopowders by condensation from the gas phase [21], which is characterized by a reduced synthesis pressure and quenching (rapid cooling) of the plasma jet. These features are aimed at limiting the particle size of synthesized nanopowder. The reduced pressure translates into reduced vapor concentrations, and quenching leads to rapid cooling and solidification of condensed particles, thereby preventing their excessive growth. The process considered in the present study is different in that the plasma jet enters open air at atmospheric pressure (therefore, the vapor concentration is higher) and quenching is lacking. These features contribute to an increase in size of synthesized particles (relative to the sizes typical of synthesis of nanopowders).

These hypotheses require further study.

Optical studies of the obtained microspheres were also carried out. Photoluminescence (PL) of erbium  $\text{Er}^{3+}$  ions in microspheres was excited through a microlens with a focal distance of 5 mm by a diode infrared laser with a wavelength of 980 nm and a power density up to  $100\ \text{kW}/\text{cm}^2$ . Microspheres featured intense PL in the visible and near infrared spectral regions. The equipment for PL spectra measurement was described in [3,4]. The obtained PL spectra are presented in Fig. 4. They contain lines around 530–550, 660, 800, and 1540 nm induced by intracenter transitions in the  $4f^{11}$ -shell of  $\text{Er}^{3+}$  ions. The dotted curve represents the PL spectrum of an individual erbium oxide particle normalized to the PL

spectrum of a microsphere. The fine structure of these lines is associated with transitions between the sublevels of Stark multiplets, which may indicate the presence of crystalline erbium oxide in both individual particles and microspheres [22]. The lines around 530, 550, 660, and 800 nm form via upconversion [1], which results in sequential absorption of two photons at a wavelength of 980 nm with subsequent radiative transition from levels  $^2H_{11/2}$ ,  $^4S_{3/2}$ ,  $^4F_{9/2}$ , and  $^4I_{9/2}$  to level  $^4I_{15/2}$ . Resonant energy transfer to an excited center from another radiative center is also possible if their concentration is high [23]. This illustrates the applicability of microspheres as a source of visible light. The broad emission band at 1455–1585 nm (corresponding to fundamental transition  $^4I_{13/2} \rightarrow ^4I_{15/2}$ ) falls within the wavelength range used in fiber communication lines [24].

The lack of cavities in microspheres is an advantage of the process under consideration. Cavities in microspheres exert a profound negative influence on their optical properties, since they will induce additional uncontrolled light scattering. In addition, the volume of emitting erbium oxide will decrease. This will have a particularly negative impact if a cavity forms in the very center of a microsphere, since our next goal is to obtain radial emission from their centers, where the bulk of energy of the electromagnetic field of the spherical Bragg microresonator is concentrated.

The produced microspheres may serve as a basis for microscopic point sources of noncoherent and coherent radiation in the visible and near IR ranges, including the wavelength of fiber communication lines (1.5  $\mu\text{m}$ ), and may also be used as converters of thermal energy into narrow-band selective radiation in the visible and IR spectral regions.

Thus, a theoretical and experimental study of processing of fine erbium oxide powder in a radio-frequency plasma jet with the aim of producing light-emitting microspheres was carried out.

Plasma processes inside an RF ICP torch and the motion of erbium oxide powder in the plasma jet were calculated. The technological process parameters ensuring efficient powder processing were determined as a result.

Experimental data demonstrated that the resulting erbium oxide microspheres are an order of magnitude larger than the original powder particles. The reason for this is not entirely clear; further research is needed.

Optical studies of the obtained microspheres revealed intense photoluminescence in the visible and near infrared spectral regions.

## Funding

This study was carried out under state assignment of the Ministry of Science and Higher Education of the Russian Federation (project FSEG-2023-0012).

## Conflict of interest

The authors declare that they have no conflict of interest.

## References

- [1] H. Guo, Y.M. Qiao, *Opt. Mater.*, **31**, 583 (2009). DOI: 10.1016/j.optmat.2008.06.011
- [2] A. Rapaport, J. Milliez, M. Bass, A. Cassanho, H. Jenssen, *J. Display Technol.*, **2** (1), 68 (2006). DOI: 10.1109/JDT.2005.863781
- [3] A.V. Medvedev, A.A. Dukin, N.A. Feoktistov, V.G. Golubev, *Tech. Phys. Lett.*, **43** (10), 885 (2017). DOI: 10.1134/S106378501710008X.
- [4] A.V. Medvedev, A.A. Dukin, N.A. Feoktistov, V.G. Golubev, *Semiconductors*, **53** (7), 901 (2019). DOI: 10.1134/S1063782619070170.
- [5] K. Imakita, H. Shibata, M. Fujii, S. Hayashi, *Opt. Express*, **21** (9), 10651 (2013). DOI: 10.1364/OE.21.010651
- [6] M. Humar, I. Musevic, *Opt. Express*, **18** (26), 26995 (2010). DOI: 10.1364/OE.18.026995
- [7] Y. Xu, W. Liang, A. Yariv, J.G. Fleming, S.-Y. Lin, *Opt. Lett.*, **29** (5), 424 (2004). DOI: 10.1364/OL.29.000424
- [8] K. Han, Y. Zhang, Z. Fang, T. Cheng, M. Gao, *Chem. Lett.*, **36** (9), 1124 (2007). DOI: 10.1246/cl.2007.1124
- [9] T.D. Nguyen, C.D. Dinh, T. Do, *ACS Nano*, **4** (4), 2263 (2010). DOI: 10.1021/nn100292s
- [10] S.V. Dresvin, A.V. Donskoy, V.M. Goldfarb, V.S. Klubnikin, *Physics and technology of low-temperature plasmas* (Iowa State University Press, Ames, USA, 1977).
- [11] S.V. Dresvin, S.G. Zverev, *Plazmotrony: konstruktivnaya parametry, tekhnologii* (Izd. Politekh. Univ., SPb., 2007) (in Russian).
- [12] M.I. Boulos, P.L. Fauchais, E. Pfender, *Handbook of thermal plasmas* (Springer International Publ., 2023). DOI: 10.1007/978-3-030-84936-8
- [13] S.V. Dresvin, S.G. Zverev, *Teploobmen v plazme* (Izd. Politekh. Univ., SPb., 2008) (in Russian).
- [14] D.V. Ivanov, S.G. Zverev, *IEEE Trans. Plasma Sci.*, **45** (12), 3125 (2017). DOI: 10.1109/TPS.2017.2773140
- [15] D.V. Ivanov, S.G. Zverev, *IEEE Trans. Plasma Sci.*, **48** (2), 338 (2020). DOI: 10.1109/TPS.2019.2957676
- [16] D.V. Ivanov, S.G. Zverev, *IEEE Trans. Plasma Sci.*, **50** (6), 1700 (2022). DOI: 10.1109/TPS.2022.3175741
- [17] D.V. Ivanov, S.G. Zverev, *Vest. Bashkir. Universiteta*, **28** (3), 222 (2023) (in Russian). DOI: 10.33184/bulletin-bsu-2023.3.2
- [18] *Vysokoskorostnaya kamera Evercam HR 2000-16-S* [Electronic source]. <https://evercam.ru/produktsiya/52/945/>
- [19] I.P. Gulyaev, O.P. Solonenko, *Thermophys. Aeromech.*, **20** (6), 769 (2013). DOI: 10.1134/S0869864313060140.
- [20] O.P. Solonenko, *Thermophys. Aeromech.*, **21** (6), 735 (2014). DOI: 10.1134/S0869864314060080.
- [21] V.Ya. Frolov, D.V. Ivanov, M.A. Shibaev, *Tech. Phys. Lett.*, **40** (8), 676 (2014). DOI: 10.1134/S1063785014080185.

- [22] G.N. Aliev, V.G. Golubev, A.A. Dukin, D.A. Kurdyukov, A.V. Medvedev, A.B. Pevtsov, L.M. Sorokin, J.L. Hutchison, *Phys. Solid State*, **44** (12), 2224 (2002). DOI: 10.1134/1.1529915.
- [23] V.V. Ovsyankin, P.P. Feofilov, *Izv. Akad. Nauk SSSR. Ser. Fiz.*, **37**, 262 (1973) (in Russian).
- [24] P.J. Winzer, D.T. Neilson, A.R. Chraplyvy, *Opt. Express*, **26** (18), 24190 (2018). DOI: 10.1364/OE.26.024190

*Translated by D.Safin*